Research Article
The Performance of the Higher-Order Radiation Condition Method for the Penetrable Cylinder

Bülent Yılmaz

We have considered the scattering of a plane wave by a penetrable acoustic circular cylinder. The boundary conditions are continuity of the total pressure and the total velocity. The wave speed and density of the target are different from that of the surrounding medium. We investigated the performance of higher-order SRCs up to L_4 operator in two dimensions. We assume that in the rectangular Cartesian system of axes, (x, y, z), the z axis coincides with the axis of the cylinder and an incident wave propagates in a direction perpendicular to the z axis. All the field quantities are then independent of z. Numerical results are added to present the change of the module of the total field and the magnitude of the far field with respect to θ.

1. Introduction

Approximate techniques have been introduced to study the scattering of waves by obstacles. The aim of these methods is to reduce the work involved in solving an integral equation or any appropriate formulation of the problem. The on-surface radiation condition (OSRC) method has been devised by Kriegsmann et al. to investigate electromagnetic scattering problems involving cylindrical convex objects [1]. The main concept in this method is the application of a radiation condition, connecting the field and its normal derivative, directly onto the surface of the scatterer to determine approximately the surface field or its derivative in terms of the given field. The calculation of the scattered field is then reduced to quadratures. As is demonstrated in [1–4] for a wide variety of two- and three-dimensional obstacles, results are in conformity with exact analysis or numerical methods over a wide range of frequencies. One of the approaches to derive radiation boundary conditions (RBCs) is based on the idea of killing the terms of the expansion of

the scattering field satisfying the Helmholtz equation and Sommerfeld radiation condition. An nth-order RBC operator which annihilates the first n terms in the expansion is obtained either on a large circular cylinder enclosing a cylindrical convex object, or on a large sphere enclosing a finite convex object, depending on the geometrical dimensions of the problem. These RBCs can be generalized so that they can be used in the OSRC method for constructing the approximate solution of a scattering problem involving an arbitrary convex object. In [1–4] only the first- and second-order RBCs have been produced and used in conjunction with the OSRC method. Later [5] third- and fourth-order RBCs have been used to examine whether the use of higher-order SRCs in the OSRC method models creeping-wave physics more accurately than a second-order SRC. Some three-dimensional canonical problems, namely, scattering by an impedance sphere and a penetrable sphere, are investigated in a variety of circumstances. The conclusion was that introduction of higher-order radiation conditions improves the approximation considerably in comparison with results obtained by the use of a second-order SRC, especially in cases in which creeping waves are less pervasive.

In this work, we employ the second- and fourth-order RBCs given by Bayliss et al. [6] in the method to investigate the scattering of a plane wave by a penetrable circular cylinder. The results obtained by the SRC method are compared with the exact result for a penetrable cylinder.

The paper is organized as follows. The formulation of the problem and the RBCs of the mode-annihilation method are presented in Section 2. In Section 3, first the exact solution of the problem is given. Then approximate solutions by the OSRC method are obtained. In Section 3, comparisons are made between the second- and fourth-order conditions via the exact results. Section 4 contains some concluding remarks.

2. Formulation

Elliptic boundary value problems governed by the Helmholtz equation in exterior regions arise in many branches of continuum physics. An example is the scattering of a time harmonic acoustic wave u^i by an obstacle occupying the region $\mathcal{B}_2$ with a boundary surface Σ_1. Let us denote the region outside Σ_1 by $\mathcal{B}_1$. If we assume that $\mathcal{B}_1$ is a homogeneous isotropic medium with sound speed c_1, constant density ρ_1, angular frequency w, and the time dependence is taken as $\exp(iwt)$, then in this region the scattered field u_1 must satisfy the Helmholtz equation

$$\nabla^2 u_1 + k_1^2 u_1 = 0, \quad k_1 = \frac{w}{c_1} \tag{2.1}$$

with boundary condition(s) specified on Σ_1. In addition, at infinity u_1 must have the form of a radiating wave, that is, the following Sommerfeld radiation condition must be satisfied:

$$\lim_{r \to \infty} r^{1/2} \left(\frac{\partial u_1}{\partial r} + ik_1 u_1 \right) = 0. \tag{2.2}$$

When the obstacle is penetrable and the region inside Σ_1, denoted by $\mathcal{B}_2$, is filled with a homogeneous isotropic fluid with sound speed c_2 and constant density ρ_2 which are different from those of the surrounding infinite medium $\mathcal{B}_1$, then the field u_2, transmitted inside Σ_1, satisfies the Helmholtz equation

$$\nabla^2 u_2 + k_2^2 u_2 = 0. \tag{2.3}$$

In this case, the solutions of (2.1) and (2.3) are subject to the following continuity conditions on Σ_1:

$$u_1 + u^i = u_2, \quad \frac{\partial}{\partial n}(u_1 + u^i) = \zeta \frac{\partial u_2}{\partial n} \quad \text{for } \mathbf{x} \in \Sigma_1, \tag{2.4}$$

where u^i represents the incident wave, $\partial/\partial n$ denotes the differentiation along the outward normal to Σ_1, and $\zeta = \rho_1/\rho_2$. If the medium inside the obstacle is inhomogeneous, $k_2 = c_1/c_2$ will be a given function of the position, that is, $k_2 = k_2(\mathbf{x})$ for $\mathbf{x} \in \mathcal{B}_2$. Also notice that when $\zeta \ll 1$ the target is nearly rigid, whereas when $\zeta \gg 1$ the target is nearly soft.

It is well known that the solution of the Helmholtz equation satisfying the Sommerfeld radiation condition can be represented by the series which is convergent in $\mathcal{B}_1$ and is given as

$$u = H_0^{(2)}(kr) \sum_{n=0}^{\infty} \frac{F_n(\theta)}{r^n} + H_1^{(2)}(kr) \sum_{n=0}^{\infty} \frac{G_n(\theta)}{r^n}, \tag{2.5}$$

where $H_0^{(2)}$ and $H_1^{(2)}$ are Hankel functions of the second kind of order 0 and 1, respectively [8]. As this expansion is difficult to work with for large values, we will use the asymptotic expansion for u as follows:

$$u \approx \sqrt{\frac{2}{\pi k r}} e^{-i(kr - \pi/4)} \sum_{n=0}^{\infty} \frac{f_n(\theta)}{r^n}. \tag{2.6}$$

To solve the problem numerically by direct methods; we must first make the region $\mathcal{B}_1$ finite. This can be done by means of a Σ_2 curve which includes Σ_1 curve and whose center is in $\mathcal{B}_2$ and has radius r_1. With these assumptions the problem is reduced to finding the solution of the Helmholtz equation on the region bounded by Σ_1 and Σ_2, the solution must satisfy the impedance condition on Σ_1 and the boundary condition must be satisfied on Σ_2 which will play the role of the Sommerfeld radiation condition. However, this condition is as yet unknown and the first thing that comes in mind is to carry the Sommerfeld condition over to Σ_2, that is,

$$\left(\frac{\partial u}{\partial r} + iku\right)_{r=r_1} = 0. \tag{2.7}$$

However, it can be easily seen that even for the first term of the expansion (2.6), (2.7) does not hold since

$$\left(\frac{\partial}{\partial r} + ik\right)\sqrt{\frac{2}{\pi k r}} e^{-i(kr - \pi/4)} f_0(\theta) = \vartheta(r^{-3/2}). \tag{2.8}$$

If the operator $L_1 = \partial/\partial r + ik + 1/2r$ is used instead of $(\partial/\partial r + ik)$,

$$L_1\left(\sqrt{\frac{2}{\pi k r}}\, e^{-i(kr - \pi/4)} f_0(\theta)\right) = 0 \tag{2.9}$$

will be found.

This result will be true for

$$\frac{e^{-i(kr)}}{\sqrt{kr}} F(\theta), \tag{2.10}$$

where $F(\theta)$ is an arbitrary function and for (2.6) the following will be valid:

$$(L_1 u)_{r=r_1} = \vartheta(r^{-5/2}). \tag{2.11}$$

That is when L_1 is applied to u, a result less erroneous than the Sommerfeld radiation condition is obtained. Higher-order boundary condition operators can be obtained by using similar arguments and they are defined by the following relations for $m > 1$ (see [2]):

$$L_m = \left(\frac{\partial}{\partial r} + ik + \frac{4m - 3}{2r}\right) L_{m-1}. \tag{2.12}$$

The first four operators in polar coordinates for the Helmholtz equations [7], used in this paper, are

$$L_1 u = \frac{\partial u}{\partial r} + iku + \frac{u}{2r} \tag{2.13}$$

$$L_2 u = 2\left(\frac{1}{r} + ik\right)\frac{\partial u}{\partial r} - \left(2k^2 + \frac{3}{4r^2} + \frac{3ik}{r}\right)u - \frac{1}{r^2}\frac{\partial^2 u}{\partial \theta^2} \tag{2.14}$$

$$L_3 u = \left(\frac{23}{4r^2} + \frac{12ik}{r} - 4k^2\right)\frac{\partial u}{\partial r} + \left(\frac{15}{8r^3} + \frac{45ik}{4r^2} - \frac{14k^2}{r} - 4ik^3\right)u$$
$$+ \left(\frac{-9}{2r^3} - \frac{3ik}{r^2}\right)\frac{\partial^2 u}{\partial \theta^2} - \frac{1}{r^2}\frac{\partial^2}{\partial \theta^2}\left(\frac{\partial u}{\partial r}\right), \tag{2.15}$$

$$L_4 u = \left(\frac{22}{r^3} + \frac{71ik}{r^2} - \frac{48k^2}{r} - 8ik^3\right)\frac{\partial u}{\partial r} + \left(\frac{105}{16r^4} + \frac{105ik}{2r^3} - \frac{94k^2}{r^2} - \frac{52ik^3}{r} + 8k^4\right)u$$
$$+ \left(\frac{-43}{2r^4} - \frac{30ik}{r^3} + \frac{8k^2}{r^2}\right)\frac{\partial^2 u}{\partial \theta^2} + \left(\frac{-8}{r^3} - \frac{4ik}{r^2}\right)\frac{\partial^2}{\partial \theta^2}\left(\frac{\partial u}{\partial r}\right) + \frac{1}{r^4}\frac{\partial^4 u}{\partial \theta^4}. \tag{2.16}$$

3. Comparison

The following equation can be written for a plane wave incident in the direction of the positive x-axis:

$$u^i = e^{-ik_1 r \cos\theta} = \sum_{n=-\infty}^{\infty} J_n(k_1 r) e^{in(\theta - \pi/2)}. \tag{3.1}$$

Let the centre of the cylinder be at the origin and let a be the radius, consider the exterior region $\mathcal{B}_1 = \{r > a\}$ and the interior region $\mathcal{B}_2 = \{r < a\}$, and a circle with $r = a$ on Σ_1. The problem is defined as

$$\nabla^2 u_1 + k_1^2 u_1 = 0 \quad (x, y) \in \mathcal{B}_1, \tag{3.2}$$

$$\nabla^2 u_2 + k_2^2 u_2 = 0 \quad (x, y) \in \mathcal{B}_2, \tag{3.3}$$

$$r = a, \quad u^i + u_1 = u_2, \quad \frac{\partial}{\partial n}(u^i + u_1) = \zeta \frac{\partial u_2}{\partial n}. \tag{3.4}$$

In addition, u_1 must satisfy the condition (2.2). The solution of Helmholtz equation for u_1 and u_2 at $\mathcal{B}_1$ and $\mathcal{B}_2$, respectively, can be written as

$$u_1 = \sum_{n=-\infty}^{\infty} a_n H_n^{(2)}(k_1 r) e^{in(\theta - \pi/2)},$$

$$\tag{3.5}$$

$$u_2 = \sum_{n=-\infty}^{\infty} b_n J_n(k_2 r) e^{in(\theta - \pi/2)}.$$

Using boundary conditions (3.4) for u_1 and u_2, we determine a_n and b_n as follows:

$$a_n = \frac{\zeta k_2 J_n'(k_2 a) J_n(k_1 a) - k_1 J_n(k_2 a) J_n'(k_1 a)}{k_1 J_n(k_2 a) H_n^{(2)'}(k_1 a) - \zeta k_2 J_n'(k_2 a) H_n^{(2)}(k_1 a)}, \tag{3.6}$$

$$b_n = - \frac{2i}{\pi a \{k_1 J_n(k_2 a) H_n^{(2)'}(k_1 a) - \zeta k_2 J_n'(k_2 a) H_n^{(2)}(k_1 a)\}}. \tag{3.7}$$

Note that if $\zeta \ll 1$ and $\zeta \to 0$, then the obstacle is almost like a hard obstacle. If $\zeta \gg 1$, then the obstacle is almost like a soft obstacle.

The radiation boundary conditions have been derived at the phase fronts and on these surfaces establish the approximate (asymptotic) relation between the derivative of u in the direction of the normal to u and its tangential derivatives. Hence these relations will be valid wherever there is a wave front. Kriegsmann et al. [1] assume that these expressions are also valid on Σ_1 and replace $\partial/\partial n$ with $\partial/\partial r$ at $L_1 u$ and $L_2 u$. Therefore, at the representation in two dimensions of the radiation boundary conditions given by (2.12)–(2.16)

replacing $\partial/\partial r$ with $\partial/\partial n$ and writing $u = u_1$, the following relation is given between normal derivative of scattering field and tangential derivative on Σ_1:

$$\frac{\partial u_1}{\partial n} = \Lambda^{(m)} u_1, \quad m = 2, 3, 4. \tag{3.8}$$

This relation is based on behavior local to a wavefront. $\Lambda^{(m)} u_1$ denotes all the terms of the radiations except the term with $\partial u/\partial r$. Boundary condition on Σ_1 from (2.4) is

$$u_1 = u_2 - u^i, \quad \frac{\partial u_1}{\partial n} = \zeta \frac{\partial u_2}{\partial n} - \frac{\partial u^i}{\partial n}. \tag{3.9}$$

Then the relation

$$\zeta \frac{\partial u_2}{\partial n} - \Lambda^{(m)} u_2 = \frac{\partial u^i}{\partial n} - \Lambda^{(m)} u^i \tag{3.10}$$

is obtained (3.3), and (3.10) defines an interior problem for u_2. For a cylinder of radius a, the second-, third- and fourth-order radiation conditions are found to be

$$\alpha_1^{(m)} \frac{d^4 v_1}{d\theta^4} + \alpha_2^{(m)} \frac{d^2 v_1}{d\theta^2} + \alpha_3^{(m)} v_1 = \alpha_4^{(m)} \frac{d^2 w_1}{d\theta^2} + \alpha_5^{(m)} w_1, \quad m = 2, 3, 4, \tag{3.11}$$

where

$$v_1(\theta) = u_1(a, \theta), \qquad w_1(\theta) = \frac{1}{k_1} \frac{\partial u_1}{\partial r}(a, \theta), \tag{3.12}$$

and $\alpha_q^{(m)}$ are functions of $\varepsilon = k_1 a$. In (3.11) the superscript m denotes the order. $\alpha_q^{(m)}$ are defined as

$$\alpha_1^{(2)} = 0, \qquad \alpha_2^{(2)} = 1, \qquad \alpha_3^{(2)} = -\frac{3}{4} - 3i\epsilon + 2\epsilon^2, \qquad \alpha_4^{(2)} = 0, \qquad \alpha_5^{(2)} = 2\epsilon(1 + i\epsilon),$$

$$\alpha_1^{(3)} = 0, \qquad \alpha_2^{(3)} = -3i\epsilon - \frac{9}{2}, \qquad \alpha_3^{(3)} = \frac{15}{8} + \frac{45}{4} i\epsilon - 14\epsilon^2 - 4i\epsilon^3,$$

$$\alpha_4^{(3)} = \epsilon, \qquad \alpha_5^{(3)} = -\epsilon \left(\frac{23}{4} + 12i\epsilon - 4\epsilon^2 \right),$$

$$\alpha_1^{(4)} = 1, \qquad \alpha_2^{(4)} = -\frac{43}{2} - 30i\epsilon + 8\epsilon^2, \qquad \alpha_3^{(4)} = \frac{105}{16} + \frac{105 i\epsilon}{2} - 94\epsilon^2 - 52i\epsilon^3 + 8\epsilon^4,$$

$$\alpha_4^{(4)} = 4\epsilon(2 + i\epsilon), \qquad \alpha_5^{(4)} = -\epsilon(22 + 71i\epsilon - 48\epsilon^2 - 8i\epsilon^3). \tag{3.13}$$

In the case of a penetrable cylinder, by defining

$$v_2(\theta) = u_2(a, \theta), \qquad w_2(\theta) = \frac{1}{k_2} \frac{\partial u_2}{\partial r} \quad \text{on } r = a, \tag{3.14}$$

the boundary conditions (2.4) can be written as

$$v_1 + v^i = v_2, \qquad k_1(w_1 + w^i) = k_2\zeta w_2. \tag{3.15}$$

Using these equations, we can now eliminate v_1 and w_1 from the SRCs given by (3.11) to obtain

$$\alpha_1^{(m)}\frac{d^4v_2}{d\theta^4} + \alpha_2^{(m)}\frac{d^2v_2}{d\theta^2} + \alpha_3^{(m)}v_2 - \frac{k_2}{k_1}\zeta\left\{\alpha_4^{(m)}\frac{d^2w_2}{d\theta^2} + \alpha_5^{(m)}w_2\right\}$$

$$= \alpha_1^{(m)}\frac{d^4v^i}{d\theta^4} + \alpha_2^{(m)}\frac{d^2v^i}{d\theta^2} + \alpha_3^{(m)}v^i - \frac{k_2}{k_1}\zeta\left\{\alpha_4^{(m)}\frac{d^2w^i}{d\theta^2} + \alpha_5^{(m)}w^i\right\}. \tag{3.16}$$

The result is an impedance-type boundary condition on $r = a$ connecting v_2 and w_2 and their tangential derivatives with the incident field. Thus u_2 is to be the solution of

$$\nabla^2 u_2 + k_2 u_2 = 0, \quad \mathbf{x} \in \mathcal{B}_2, \tag{3.17}$$

which satisfies this resulting impedance boundary condition on $r = a$. Notice that (3.16) and (3.17) constitute an interior elliptic boundary value problem. Once u_2 has been determined, v_1 and w_1 are found from (3.15). Applying the method of separation of variables, the solution of (3.17) is obtained as

$$u_2 = \sum_{n=-\infty}^{\infty} B_n J_n(k_2 r) e^{in(\theta - \pi/2)} \tag{3.18}$$

and the use of the boundary condition (3.16) yields

$$B_n = \frac{\Theta^{(m)}(\varepsilon)J_n(\varepsilon) - J'_n(\varepsilon)}{\Theta^{(m)}(\varepsilon)J_n(k_2 a) - (k_2/k_1)\zeta J'_n(k_2 a)}, \tag{3.19}$$

where

$$\Theta^{(m)}(\varepsilon) = -\frac{n^4\alpha_1^{(m)} - n^2\alpha_2^{(m)} + \alpha_3^{(m)}}{n^2\alpha_4^{(m)} - \alpha_5^{(m)}}. \tag{3.20}$$

The exact solution of the problem is also given by (3.18), on replacing $\Theta_n^{(m)}(\varepsilon)$ by $H_n^{(2)'}(\varepsilon)/H_n^{(2)}(\varepsilon)$ in (3.19). Thus, for the problem under consideration the SRCs method is equivalent to introducing the approximation

$$\frac{H_n^{(2)'}(\varepsilon)}{H_n^{(2)}(\varepsilon)} \approx \Theta^{(m)}(\varepsilon), \tag{3.21}$$

and therefore, this result is independent of the boundary conditions prescribed on the surface of the circular cylinder Σ_1. Hence, the accuracy of the method for the cylinder problems will depend on the accuracy of the approximation in (3.21).
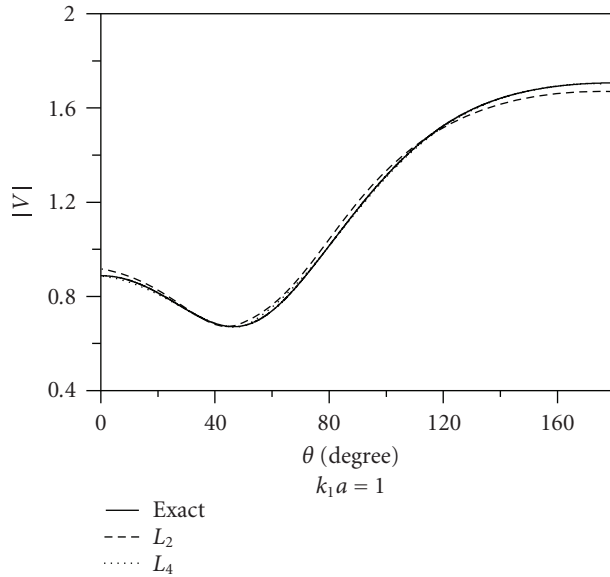
(a)
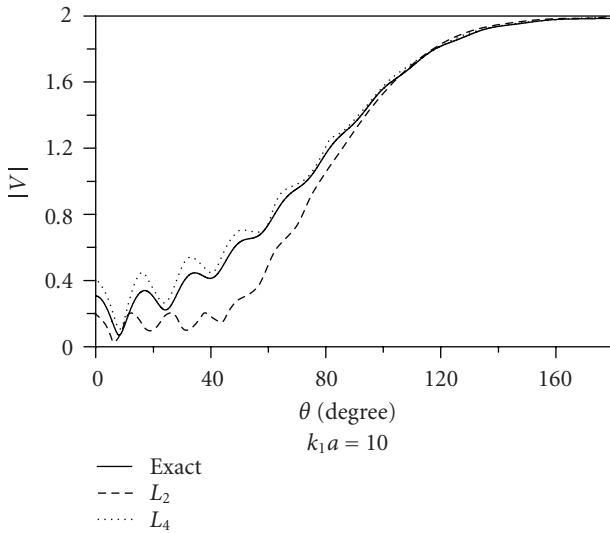
(b)

Figure 3.1

If, at $r = a$, namely, over Σ_1, relations $u^t(a,\theta) = v_2(\theta)$, $(\partial u^t/\partial r)(a,\theta) = k_2\xi_1 w_2(\theta)$, and $\mathcal{K}(\mathbf{x},\mathbf{y}) = -(1/4)iH_0^{(2)}(k_1|\mathbf{x} - \mathbf{y}|)$ are used in the following integral representation:

$$u^i(\mathbf{x}) + \int_{\Sigma_1} \left\{ \frac{\partial u^t(\mathbf{y})}{\partial n_y}\mathcal{K}(\mathbf{x},\mathbf{y}) - u^t(\mathbf{y})\frac{\partial}{\partial n_y}\mathcal{K}(\mathbf{x},\mathbf{y}) \right\} ds_y = u^t(\mathbf{x}), \quad \mathbf{x} \in \mathcal{B}_1, \qquad (3.22)$$

the scattered field in any point in the region $\mathcal{B}_1$ is obtained by calculating the following integral [9]:

$$
\begin{aligned}
u_1(r,\theta) = \frac{i}{4} \int_0^{2\pi} &\left[v_2(\theta') \frac{\partial}{\partial a} H_0\{k_1(r^2 + a^2 - 2ra\cos(\theta - \theta'))^{1/2}\} \right. \\
&\left. - k_2\xi_1 w_2(\theta') H_0\{k_1(r^2 + a^2 - 2ra\cos(\theta - \theta'))^{1/2}\} \right] ad\theta'.
\end{aligned}
\tag{3.23}
$$

Thus the amplitude of the far field is obtained as follows:

$$
P(\theta) = \frac{i\varepsilon}{4} \int_0^{2\pi} \left\{ v_2(\theta') i\cos(\theta - \theta') - \frac{k_2}{k_1} \xi_1 w_2(\theta') \right\} e^{i\varepsilon\cos(\theta - \theta')} d\theta'.
\tag{3.24}
$$

Here if (3.3) is used and the expressions $\int_0^{2\pi} e^{i\varepsilon\cos(\theta-\theta')+in(\theta'-\pi/2)} d\theta' = 2\pi J_n(\varepsilon) e^{in\theta}$ and $\int_0^{2\pi} \cos(\theta-\theta') e^{i\varepsilon\cos(\theta-\theta')+in(\theta'-\pi/2)} d\theta' = -i2\pi J_n'(\varepsilon) e^{in\theta}$ are considered, the amplitude of the far field is obtained as follows:

$$
P(\theta) = \frac{i\varepsilon\pi}{2} \sum_{n=-\infty}^{\infty} C_n e^{in\theta}.
\tag{3.25}
$$

Here again C_n is expressed as follows:

$$
C_n = \left\{ J_n'(\varepsilon) J_n(k_2 a) - \frac{k_2\xi}{k_1} J_n(\varepsilon) J_n'(k_2 a) \right\} B_n.
\tag{3.26}
$$

For the exact solution, the amplitude of the far field is calculated from

$$
P^{\text{exact}}(\theta) = \sum_{n=-\infty}^{\infty} a_n e^{in\theta},
\tag{3.27}
$$

where a_n is given in (3.6). If we compare (3.25) and (3.27), the method gives the approximation $(i\varepsilon\pi/2)C_n \sim a_n$. If we substitute $H_n^{(2)'}(\varepsilon)/H_n^{(2)}(\varepsilon)$ instead of $\Theta^{(m)}(\varepsilon)$ in (3.19), we obtain $(i\varepsilon\pi/2)C_n = a_n$. Thus, the approximation (3.21) is also valid for the far field.

4. Conclusion

Comparisons are made between the exact answer of the problem and the SRC solutions. Numerical results for the variation of the modules of the total surface field with θ and the variations of the modules of far field, namely, of scattering function P with respect to θ are presented for various values of ka. It is observed that introduction of higher-order radiation conditions improve the approximation considerably in comparison to results obtained by the use of the second-order radiation condition, especially in cases where creeping waves are less pervasive.
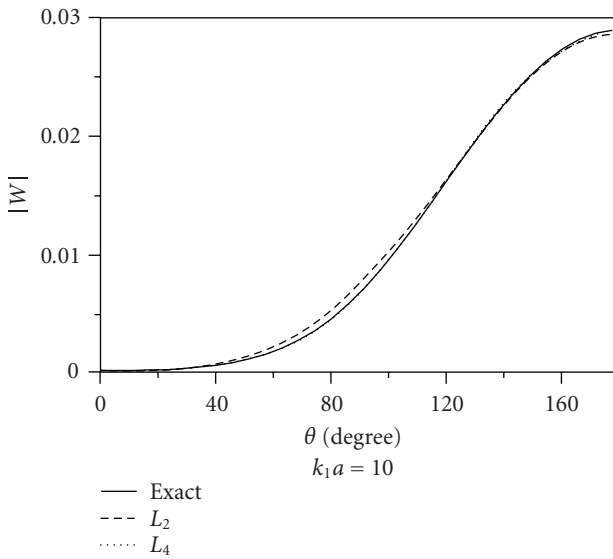
The parameters used are as follows.

(A) $\rho_1 = 1.2$, $c_1 = 340$, $\rho_2 = 1000$, $c_2 = 1480$, $k_2 = c_1 k_1/c_2$ (if there is water in B_2 and air in $\mathcal{B}_1$).

(B) $\rho_1 = 1000$, $c_1 = 1480$, $\rho_2 = 1.2$, $c_2 = 340$, $k_2 = c_1 k_1/c_2$ (if there is air in B_2 and water in $\mathcal{B}_1$).
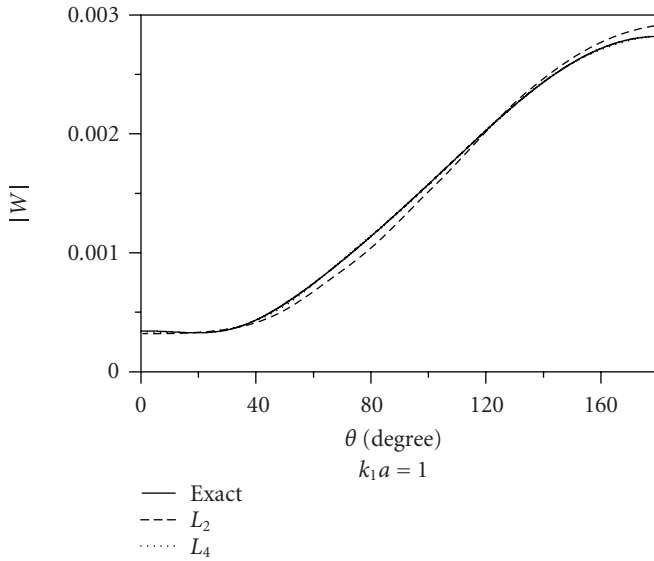
(a)

(b)

Figure 3.2

In Figure 3.1, the results of the second- and fourth-order SRCs for the parameters given in (A) (nearly hard cylinder) are depicted together with the exact curve for $k_1a = 1$ and 10. It can be seen that the fourth-order SRC improves the method and gives better results than the second-order SRC.
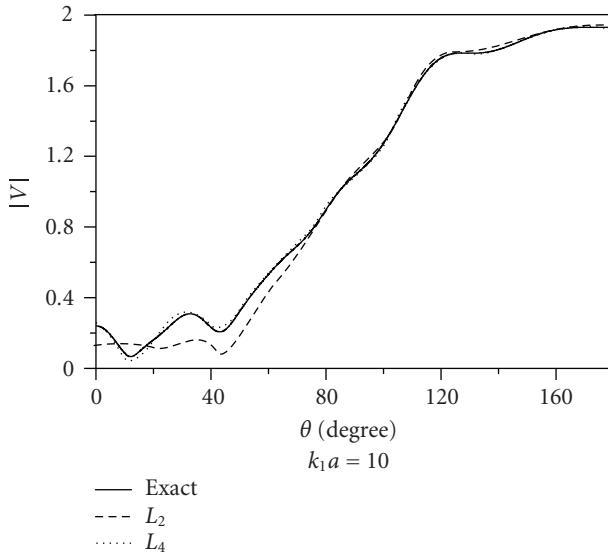
Exact

--- L_2

...... L_4
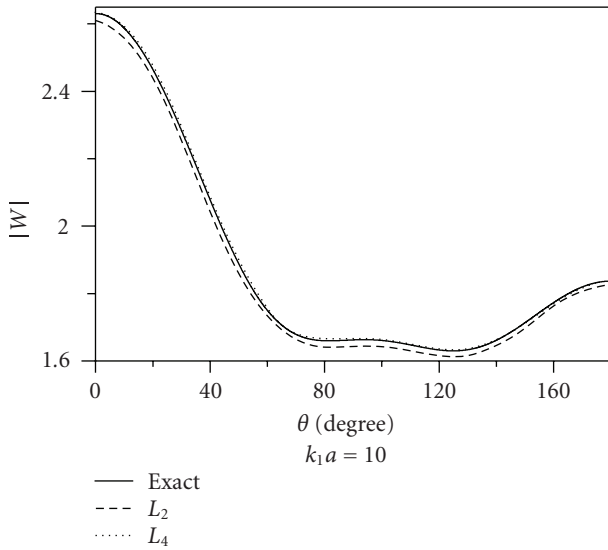
Figure 3.3

Exact

--- L_2

...... L_4

Figure 3.4

In **Figure 3.2**, the results of the second- and fourth-order SRCs for the parameters in (B) (nearly soft cylinder) for $k_1 a = 1$ and 10 are depicted together with exact ones. It can be seen that for both $k_1 a = 1$ and 10 the performance of the fourth-order SRC is perfect. It offers a good improvement, although the second-order SRC also produces quite good results. It should be noted that in cases given in the graphs the penetrable cylinder behaves nearly like a soft cylinder.
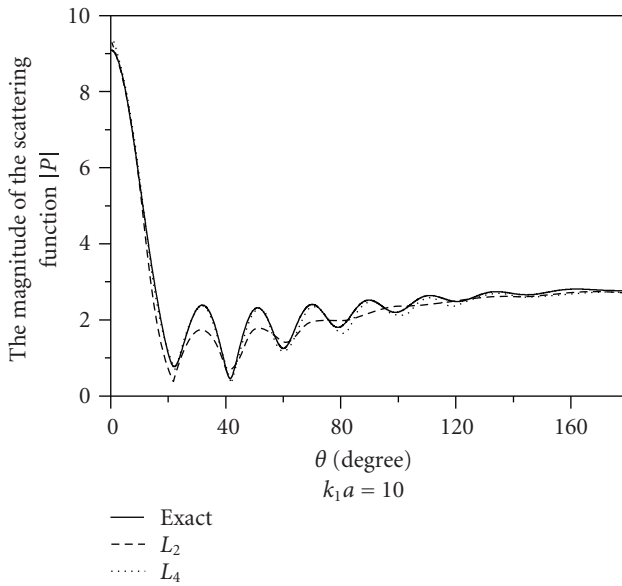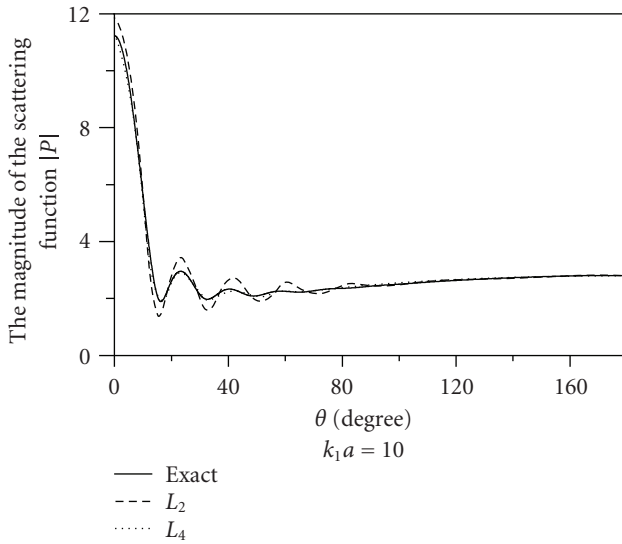
Figure 3.5

Figure 3.6

In a different manner from A and B whenever the densities of two regions are similar and the density of the smaller second region is greater than this, the case specific parameters and Figure 3.3 for $k_1a = 10$ are as follows.

(C) $\rho_1 = 1.2$, $c_1 = 340$, $\rho_2 = 2.4$, $c_2 = 800$, $k_2 = c_1 k_1/c_2$ (if there is water in B_2 and air in $\mathcal{B}_1$).

Whenever the densities of two regions are similar between them and lower than the second region, the case specific parameters and Figure 3.4 for $k_1 a = 10$ are as follows.

(D) $\rho_1 = 1200$, $c_1 = 1600$, $\rho_2 = 600$, $c_2 = 800$, $k_2 = c_1 k_1 / c_2$ (if there is air in B_2 and water in $\mathcal{B}_1$).

It can be seen from Figures 3.1 and 3.2 that the fourth-order SRC produces the most accurate results for all of the frequencies for both (A) and (B). In Figures 3.3 and 3.4, we see almost the same results of the problem according to the parameters in C and D as in A and B, respectively.

It should be noted here that in the case of B, with increasing frequency, the modules of the surface field predicted by the method becomes remarkably close to the exact answer in shadow part. This is due to the fact that creeping waves are less pervasive for soft objects and therefore the results are more accurate in the high-frequency range. Nevertheless, the fourth-order SRC improves the SRC approximation considerably for both (A) and (B) and also for all frequencies.

Here in a similar way the scattered field calculations are made for the cases A, B, C, and D. In the graphics, only the calculations for A and B are plotted for $ka = 10$ because it is clear that the scattered field will show a similar attitude for C and D.

Nevertheless, as can be observed from Figure 3.5, where the magnitude of the scattering function is presented for $ka = 10$ together with the exact ones, the results are qualitatively quite satisfactory. The magnitude of the scattering function becomes less accurate in the forward region.

The attitude of the scattered field in Figure 3.6 has a similar attitude to that of Figure 3.5.

The analysis presented here is restricted to a special problem. However, it is likely that similar behavior occurs in scattering problems for arbitrary convex objects with the boundary condition. The analysis of such problems will be more complicated, but this above-mentioned concrete example provides valuable information about the capability of the method to deal with them.

Acknowledgment

References

[1] G. A. Kriegsmann, A. Taflove, and K. R. Umashankar, "A new formulation of electromagnetic wave scattering using an on-surface radiation boundary condition approach," *IEEE Transactions on Antennas and Propagation*, vol. 35, no. 2, pp. 153–161, 1987.

[2] M. Teymur, "A comparative investigation of the surface radiation condition in electromagnetics," *Wave Motion*, vol. 16, no. 1, pp. 1–21, 1992.

[3] G. A. Kriegsmann and T. Moore, "An application of the on-surface radiation condition to the scattering of acoustic waves by a reactively loaded sphere," *Wave Motion*, vol. 10, no. 3, pp. 277–284, 1988.

[4] S. Arendt, K. R. Umashankar, A. Taflove, and G. A. Kriegsmann, "Extension of on-surface radiation condition theory to scattering by two-dimensional homogeneous dielectric objects," *IEEE Transactions on Antennas and Propagation*, vol. 38, no. 10, pp. 1551–1558, 1990.

[5] M. Teymur, "A note on higher-order surface radiation conditions," *IMA Journal of Applied Mathematics*, vol. 57, no. 2, pp. 137–163, 1996.

[6] A. Bayliss, M. Gunzburger, and E. Turkel, "Boundary conditions for the numerical solution of elliptic equations in exterior regions," *SIAM Journal on Applied Mathematics*, vol. 42, no. 2, pp. 430–451, 1982.

[7] B. Yilmaz, "The performance of the OSRC method for concentric penetrable circular cylinder," *Journal of Mathematical Physics*, vol. 47, no. 4, Article ID 043515, 11 pages, 2006.

[8] S. N. Karp, "A convergent 'far-field' expansion for two-dimensional radiation functions," *Communications on Pure and Applied Mathematics*, vol. 14, no. 3, pp. 427–434, 1961.

[9] D. S. Jones, *Acoustic and Electromagnetic Waves*, Oxford Science Publications, The Clarendon Press, Oxford University Press, New York, NY, USA, 1986.

Bülent Yılmaz: Department of Mathematics, Faculty of Science and Letters, Marmara University, Göztepe, Kadiköy, 34722 Istanbul, Turkey
Email address: bulentyilmaz@marmara.edu.tr

Special Issue on
Time-Dependent Billiards

Call for Papers

This subject has been extensively studied in the past years for one-, two-, and three-dimensional space. Additionally, such dynamical systems can exhibit a very important and still unexplained phenomenon, called as the Fermi acceleration phenomenon. Basically, the phenomenon of Fermi acceleration (FA) is a process in which a classical particle can acquire unbounded energy from collisions with a heavy moving wall. This phenomenon was originally proposed by Enrico Fermi in 1949 as a possible explanation of the origin of the large energies of the cosmic particles. His original model was then modified and considered under different approaches and using many versions. Moreover, applications of FA have been of a large broad interest in many different fields of science including plasma physics, astrophysics, atomic physics, optics, and time-dependent billiard problems and they are useful for controlling chaos in Engineering and dynamical systems exhibiting chaos (both conservative and dissipative chaos).

We intend to publish in this special issue papers reporting research on time-dependent billiards. The topic includes both conservative and dissipative dynamics. Papers discussing dynamical properties, statistical and mathematical results, stability investigation of the phase space structure, the phenomenon of Fermi acceleration, conditions for having suppression of Fermi acceleration, and computational and numerical methods for exploring these structures and applications are welcome.

To be acceptable for publication in the special issue of Mathematical Problems in Engineering, papers must make significant, original, and correct contributions to one or more of the topics above mentioned. Mathematical papers regarding the topics above are also welcome.

Authors should follow the Mathematical Problems in Engineering manuscript format described at http://www.hindawi.com/journals/mpe/. Prospective authors should submit an electronic copy of their complete manuscript through the journal Manuscript Tracking System at http://mts.hindawi.com/ according to the following timetable:

Manuscript Due	March 1, 2009
First Round of Reviews	June 1, 2009
Publication Date	September 1, 2009

Guest Editors

Edson Denis Leonel, Department of Statistics, Applied Mathematics and Computing, Institute of Geosciences and Exact Sciences, State University of São Paulo at Rio Claro, Avenida 24A, 1515 Bela Vista, 13506-700 Rio Claro, SP, Brazil; edleonel@rc.unesp.br

Alexander Loskutov, Physics Faculty, Moscow State University, Vorob'evy Gory, Moscow 119992, Russia; loskutov@chaos.phys.msu.ru